

CONTRIBUTIONS REGARDING THE NARROW GAP MAG WELDING PROCESS OF STEEL INTENDED TO GAS PIPELINES EXECUTIONS

PhD thesis – Summary

To obtain the scientific title of doctor at
Polytechnic University of Timișoara
in the field of Material engineering

author ing. Dinu SIMIONESCU

scientific leader: Prof.univ.dr.ing. Ion MITELEA

luna februarie anul 2022

Chapter 1

CURRENT STATE OF RESEARCH ON WELDING BEHAVIOR OF STEEL FOR MAIN PIPELINES

1.1. Introduction

Currently worldwide, the demand for the transport of oil and natural gas products is constantly growing. For the transport of these products, new underground and submarine main pipeline networks are being developed. The costs of making these types of pipes are quite high, which is why, worldwide, extensive research is carried out in the following directions:

- the use of steel pipes for main pipelines made of high-strength steels, which leads to a reduction in wall thickness, so to a lower consumption of welding consumables;
- development of high efficiency welding technologies;
- implementation of automatic control methods.

For non-alloy steels, the increase in mechanical properties cannot be achieved by increasing the carbon concentration, as this results in a decrease in toughness, ductility and weldability. Therefore, the increase of the mechanical characteristics will be done by one of the following processes [1],[20],[33],[40],[51],[58],[84],[86],[104]:

- fine grains;
- hardening of the solid solution by microalloys;
- hardening by dispersed precipitation;
- increasing the density of dislocations.

1.4. Elements of difficulty of the problematic addressed

The main pipelines are designed to transport natural gas under pressure, products that are rich in hydrogen sulfide. Due to the high pressures and the toxic environment used to transport natural gas, these welding technologies and the control of welded joints require special attention from researchers.

Traditional welding of main pipelines of high thickness and lengths of hundreds and thousands of kilometers using the manual welding process with coated electrodes is not recommended due to both low productivity and high cost compared to fully automatic welding

of pipelines. Also, the use of cellulosic electrodes (electrodes that introduce a large amount of hydrogen) in the manual welding of pipelines of medium and high thickness is not recommended by any manufacturer of welding materials due to the risk of cracking caused by the presence of hydrogen.

MAG Welding (Metal Active Gas). The use of narrow gap MAG welding requires special precautions to ensure that the tip of the wire is precisely positioned to ensure proper melting of the faces of the welding joint [4],[36],[78],[103]. The narrow gap MAG welding using a single welding head is the dominant technique and has been optimized in the past to produce maximum productivity using this welding process. The continuous development of MAG welding using two welding heads and the use of MAG welding at the root leads to a significant increase in productivity [71],[80].

Welding of main pipelines and non-destructive testing are governed by API 1104 [89]. The behavior at stress corrosion cracking will be done according to the NACE TM0177 standard, Method B [88], and the preparation and bending of the samples for the corrosion test according to the ASTM G39 standard [102].

The paper aims to find a way to limit undesired microstructural transformations in the areas of welded joints, while increasing productivity by implementing a narrow gap MAG welding process of a thermo mechanically treated steel that is intended for the execution of pipelines for the oil and gas industry. It provides additional knowledge on the proper selection of welding materials, the homologation of welding technology in view of a substantial increase in productivity by using both automatic internal root welding and by using two welding heads to fill the joint at the same time with a reduction of the consumption of welding consumables due to the narrow joint.

1.5. The objectives of the doctoral thesis

Difficulties reported in narrow gap MAG welding require extensive experimental research to achieve the following objectives:

- 1.** Opportunity to make welded joints of pipes with a diameter of 42 " (1066.8 mm) from high-strength, low-carbon micro-alloy steels, thermomechanically treated (TTM), API 5LX65M, using the MAG process in arc spray for root pass and pulsed current to fill the joint. The welding equipment used will consist of a internal welding machine and two welding machines on the outside of the pipe, each with two welding torches for filling, at which the pipe is fixed and the equipment has a vertical orbital motion descent around the pipe.
- 2.** Establishment of the technological parameters of the thermal welding regime for the root and for the filling layers.
- 3.** Selection of filler materials compatible with the base metal leading to a deposited metal with favorable characteristics; thus, the option of using an ER 70S-G wire will be chosen for root welding, and for filling, the E70S-6 wire.
- 4.** Evaluation of the quality of welded joints by microscopic structure investigations, mechanical tests (hardness, static tensile, impact, cold bending) and by non-destructive testing (magnetic particles, x-rays) with the establishment of guidelines to be considered to avoid possible defects in a particular case of joining such steels.

Chapter 2

EXPERIMENTAL RESEARCH ON THE PARAMETERS OF THE WELDING PROCESS

2.1. Particularities of the narrow gap MAG welding process

The MAG welding process uses an electric arc between a fusible electrode in the form of a wire and the metal bath, the protection being made by an external source of active gas or inert gas mixtures with active gases [10],[18],[103].

It is used to join pipes, main pipelines, pressure vessels, shipyard constructions, etc.

Narrow gap MAG welding is a multi-pass welding technique used to join especially high-thickness metallic materials using I or V bevels with an angle below 10° and a joint opening of 6-16 mm.

The basic features of this process are:

- Narrow joint, the faces of the joint are parallel or slightly open;
- Reduced deformations due to the shape of the joint;
- Welding with multiple layers with one or two passes on the layer;
- In general, the heat affected zone (HAZ) is reduced due to welding with low linear energy;

2.2. Leading the experimental program

The main pipeline with a diameter of 42 " (1066.8mm) and a wall thickness of 31.75mm, made of high-strength micro-alloy steel API5L X65M, thermo mechanically treated were welded by the MAG process in spray arc for the root & hot pass and pulsed current for filling the joint using the welding equipment of CRC Evans. This consists of an internal welding machine, IWM and two externals welding machines, P625, each with two welding torches, at which the pipe is fixed and the welding equipment has a vertical downhill orbital motion around the pipe.

Prior to assembly, the ends of the pipes are machined to obtain a narrow joint (fig.2.12).

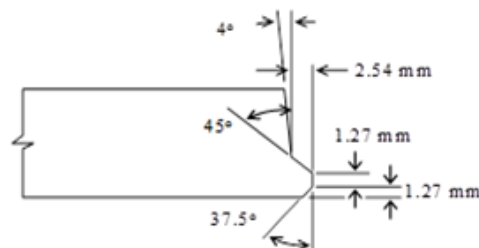


Fig.2.12 The shape and dimensions of the joint

2.3. Characterization of base metal and auxiliary material

2.3.1 Characterization of the base metal

There are numerous methods of thermo mechanical treatment, three of them being illustrated in fig.2.16. The first two (type I and II fig.2.16) do not contain an accelerated cooling from the deformation end temperature and differ from each other mainly by the temperature range in which this process takes place. The third method (type III fig.2.16) comprises an accelerated cooling after the controlled rolling process [68], [69], [104].

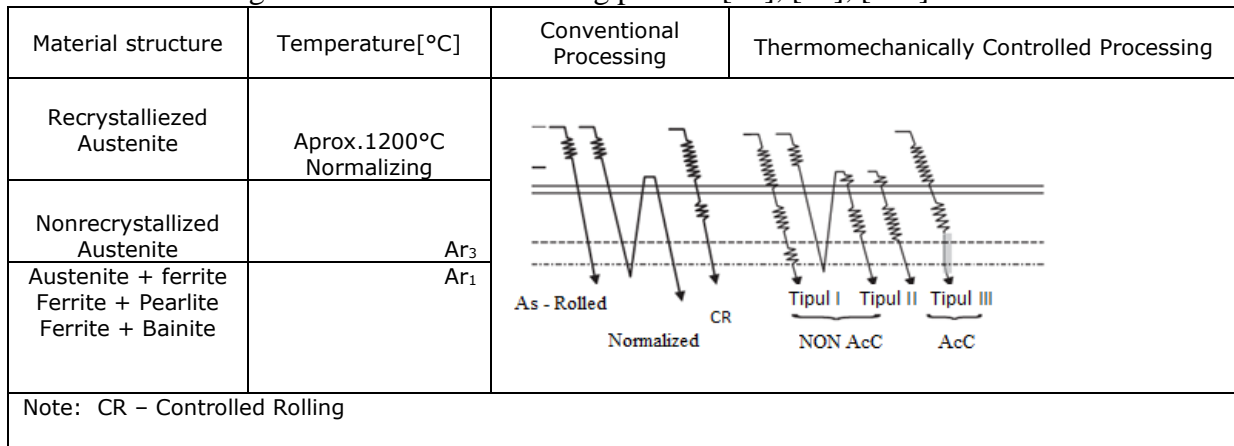


Fig. 2.16. Comparison between the conventional process and the thermomechanically controlled process

The chemical composition of the base metal used in the experiments is given in tab.2.1.

Tab.2.1 Chemical composition of the base metal : API 5L X65M

X65M	C%	Si%	P%	S%	Cu %	Ti%	Mn %	Ni %	Cr %	Al %	Mo %	V%	Nb%	B%
Actual values	0.04 3	0.32	0.0 07	0.00 09	0.02	0.01 3	1.53	0.01 8	0.19	0.03 8	0.00 8	0.0 04	0.04 4	0.00 02
Composition as per API 5L	0.1	0.4	0.0 16	0.00 2	0.35	0.04	1.6	0.3	0.3	0.06	0.15	0.0 8	0.05	0.00 05

Obs. API Specification 5L: Specification for Pipe Line (API 2018) – American Petroleum Institute [90].

2.3.2 Characterization of the auxiliary material

Tab.2.2 Chemical composition of the welding wire for the root pass, ER70S-G

ER 70S-G	C%	Si%	Mn%	P%	S%	Cr%	Mo%	Ni%	Cu%	V%	Ti%
Actual values	0.07	0.74	1.57	0.013	0.008	0.04	0.01	0.04	0.11	0.01	0.05

Note: ASME Sect.II Part C does not specify the chemical composition [92]

Tab.2.3 Chemical composition of the welding wire for the filling layers, ER70S-6

ER 70S-6	C%	Si%	Mn%	P%	S%	Cr%	Mo%	Ni%	Cu%	V%	Ti%
Actual values	0.07	0.95	1.69	0.011	0.010	0.03	0.01	0.05	0.10	0.01	<0.01
Composition prescriptions	0.06- 0.15	0.8- 1.15	1.4- 1.85	0.025	0.035	0.15	0.15	0.15	0.50	0.03	-

Note: Chemical composition as per ASME Sect.II Part C [92]

General Note: The singular values represent the maximum values of each component element

For the narrow gap MAG welding of the API 5L X65 material, the gas mixture used for both internal and external pipeline welding was: 80% Ar + 20% CO₂.

Chapter 3

STRUCTURE AND MECHANICAL PROPERTIES OF NARROW GAP MAG WELDED JOINTS

3.1. Macrography of welded joints

Fig.3.3 shows the macroscopic image of a cross section through the welded joint, noting that both the seam and the ZIT have a proper geometry and are free of defects such as porosity, cracks, lack of fusion, etc. The width of the ZIT is uniform over the entire section, and the direction of crystallization in the weld is the natural one, that is, it coincides with the direction of heat dissipation.

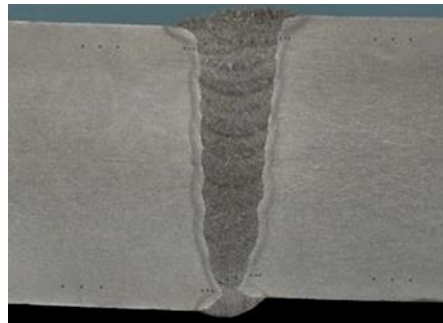


Fig.3.3 Macroscopic image of the cross section through the welded joint. Chemical reagent: NITAL (10 cm³ HNO₃, 100 cm³ ethyl alcohol)

3.2. Micrographic examinations

Microscopic investigations on the areas of the welded joint show that a dendritic structure is formed in the weld, the growth of the grains occurring in a columnar manner fig.3.6, and in ZIT appears a ferrito-bainitic structure with fine precipitation of secondary phases, fig.3.7. The base metal has a ferrito-bainitic microstructure, fig.3.8.

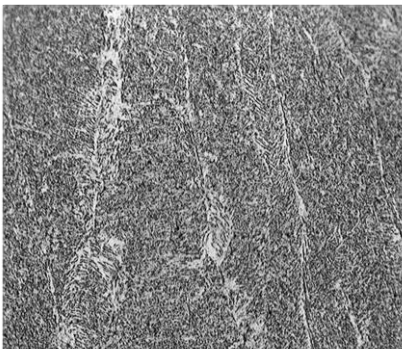


Fig.3.6 Welding microstructure, x 200

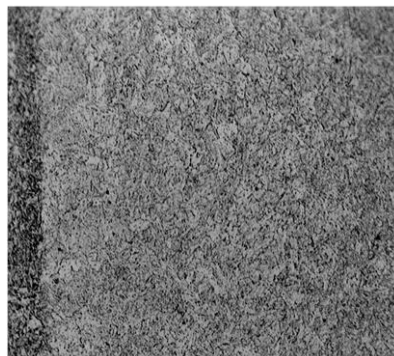


Fig.3.7 HAZ microstructure, x 200

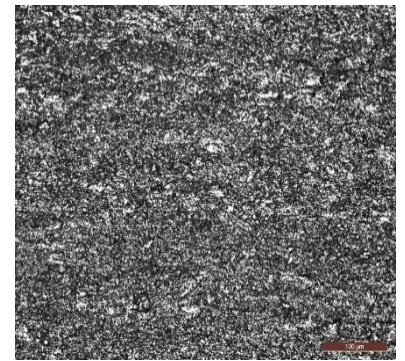


Fig.3.8 Base metal microstructure, x 200

Vickers hardness measurements on the cross section of the welded joint were performed at a distance of 2 mm from the inner part, fig.3.13, respectively the upper part, fig.3.14 of the pipe. Their degree of scattering confirms the structural heterogeneities of welding and HAZ. Slightly higher weld hardness values are explained by the slightly higher carbon equivalent content of the deposited metal compared to the base metal.

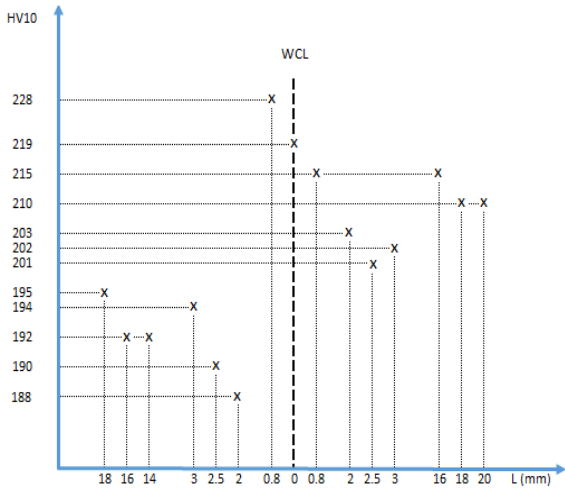


Fig.3.13 Hardness variation on the welded joint section in the internal area of the pipe

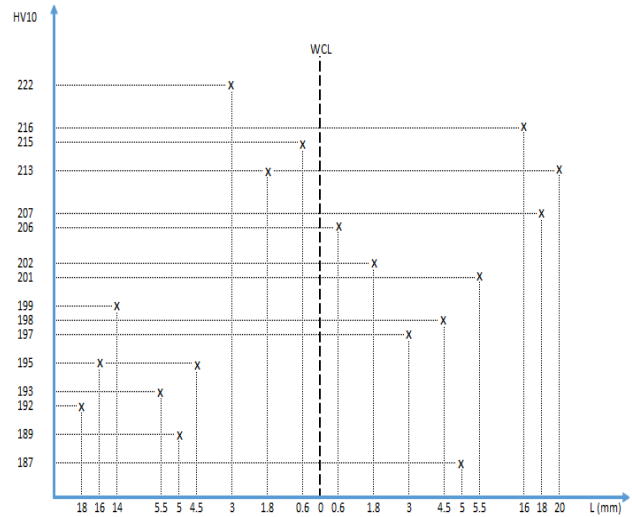


Fig.3.14 Hardness variation on the welded joint section in the outside area of the pipe

3.4. Charpy Impact testing

At least 3 specimens were used for each test temperature and each notch location. The obtained results are presented in tab.3.1 and 3.2 and represented graphically in fig.3.21 and 3.22

Tab. 3.1 The values of absorbed energy KV in welding joint

Notch location	Specimen size, mm	Temp. °C	Absorbed Energy, Joules			
			A	B	C	Average
WCL, Upper area	10 x 10 x 55	+20°	178	176	190	181
WCL, Lower area	10 x 10 x 55	+20°	220	220	208	216
WCL, Upper area	10 x 10 x 55	0°	150	138	150	146
WCL, Lower area	10 x 10 x 55	0°	198	188	226	204
WCL, Upper area	10 x 10 x 55	-30°	102	110	116	109
WCL, Lower area	10 x 10 x 55	-30°	130	150	138	139
WCL, Upper area	10 x 10 x 55	-50°	80	50	62	64
WCL, Lower area	10 x 10 x 55	-50°	44	56	50	50

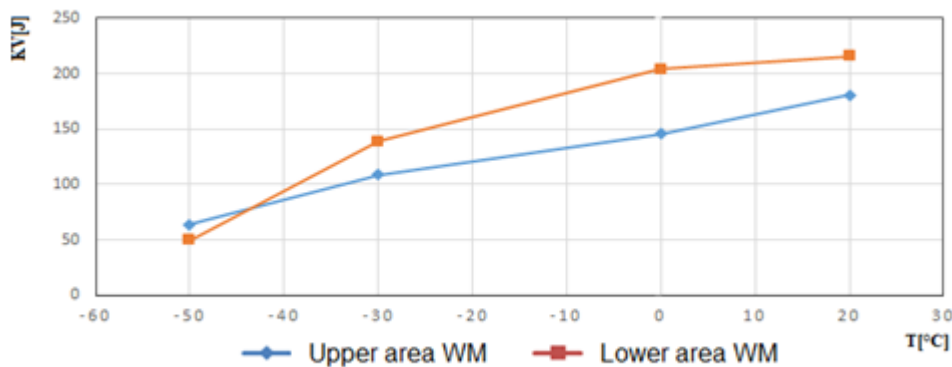


Fig.3.21 Absorbed energy variation KV with the test temperature T [°C] in welding joint

Tab. 3.2 The values of absorbed energy KV in HAZ

Notch location	Specimen size , mm	Temp. °C	Absorbed Energy , Joules			
			A	B	C	Average
HAZ, Upper area	10 x 10 x 55	+20°	N	N	N	>300
HAZ, Lower area	10 x 10 x 55	+20°	N	N	N	>300
HAZ, Upper area	10 x 10 x 55	0°	N	N	N	>300
HAZ, Lower area	10 x 10 x 55	0°	N	N	N	>300
HAZ, Upper area	10 x 10 x 55	-30°	N	N	N	>300
HAZ, Lower area	10 x 10 x 55	-30°	N	N	N	>300
HAZ, Upper area	10 x 10 x 55	-50°	162	185	175	174
HAZ, Lower area	10 x 10 x 55	-50°	144	180	210	178

Note: N – Specimen did not break

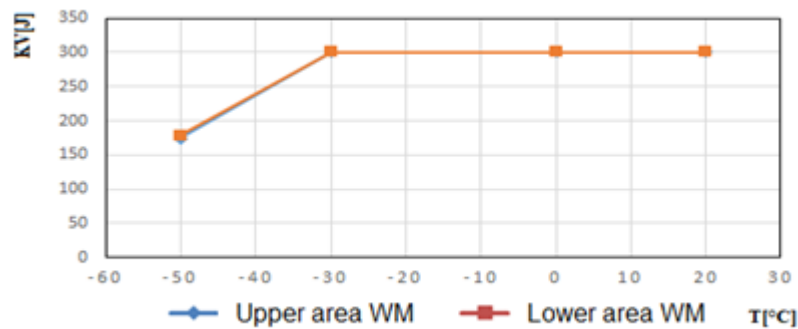


Fig.3.22 Absorbed energy variation KV with the test temperature T [°C] in HAZ

Analyzing the variation of the absorbed energy KV depending on the test temperature fig.3.21 and 3.22, it can be seen that the welded joint and HAZ have a high resistance to brittle rupture, their behavior being ductile in a wide range of temperatures (- 50 ° C - + 20 ° C).

3.5. Tensile strength test

The results of the tensile tests are presented in table 3.3, and the appearance of a tested specimen is shown in fig.3.28.

Tab.3.3 Experimental results

Specimen ID	So (mm ²)	Fmax (N)	Rm (N/mm ²)	Fracture location
TT1	800.87	476226	595	Base metal
TT2	796.45	476126	598	Base metal
TT3	801.24	469729	586	Base metal
TT4	799.22	460440	576	Base metal



Fig.3.28 Fracture location of the tensile strength test specimen

The analysis of the obtained data demonstrates that, each time, the fracture occurred in the base material (MB) and that the values of tensile strength for all 4 sets of welded specimens are higher than the minimum required for the base material (according to API 104, 2013), which is 535 N/mm².

3.6. Side bend test

The results of the side bend test are presented in tab.3.4, noting that until the 180° no cracks have been observed.

Tab. 3.4 Test conditions and results

Specimen ID	Mandrel diameter (mm)	Bend angle (°)	Results
SB1	90	180	Acceptable
SB2	90	180	Acceptable
SB3	90	180	Acceptable
SB4	90	180	Acceptable
SB5	90	180	Acceptable
SB6	90	180	Acceptable
SB7	90	180	Acceptable
SB8	90	180	Acceptable

The appearance of the welded specimen and side bend tested is shown in fig. 3.34.

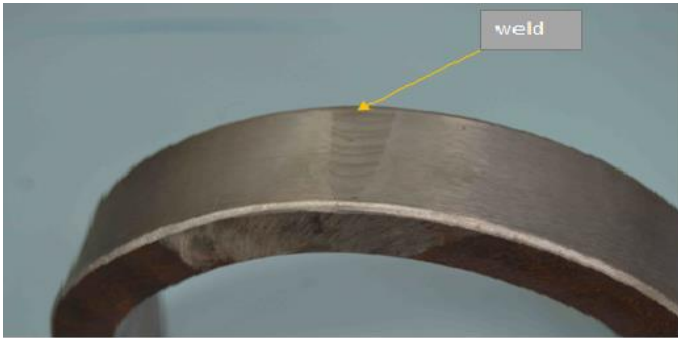


Fig.3.34 The image of side bend test specimen

3.7. Bending test of specimens with notch

Macroscopic appearance of the test specimens with notch after cold bending are exemplified in fig. 3.38.

It is noted that specimens rupture is preceded by significant plastic deformation and that no metallic continuity defects have been observed.



Fig.3.38 Macrographic specimens with notch, API 5L X65M, 42 "(1066.8mm) x31.75mm after testing

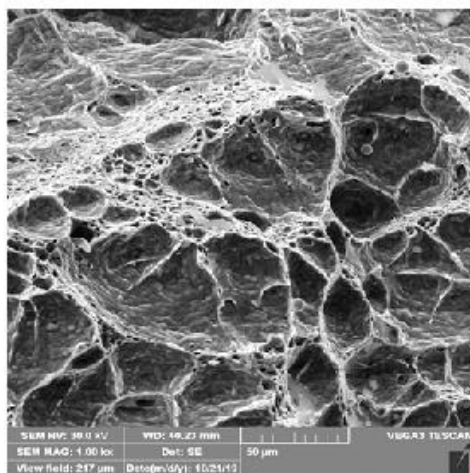
3.8. Fracture toughness of welding joints

Prediction of an unstable fracture or increase of a pre-existing crack is the fundamental problem in the mechanics of fracture (fractures) [2], [7], [12], [31], [47], [49], [54], [57], [85]. Experimental measurement of the propagation force (conduction) of a pre-existing crack obtained by fatigue plays an important role in this prediction. Stress intensity factor at the crack tip (K_{IC}), crack tip opening displacement (CTOD) and the crack tip opening angle (CTOA) are the most recognized parameters used in fracture mechanics [17], [29], [65], [75], [99], [100] [105], [106], [107], [108], [113].

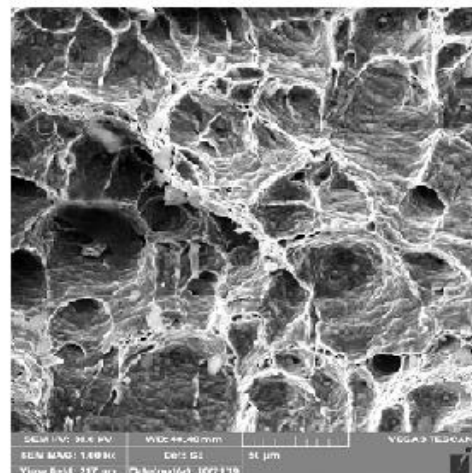
The critical values of the crack tip opening displacement (δ_m) or CTOD are presented in tab.3.11, they demonstrate that the MAG welded joints of thermo mechanically treated X65M steel have a high resistance to brittle rupture. The microfractographic images of fig. 3.56 highlights the presence of more or less rectilinear parallel streaks, next to the ductile cleavage areas corresponding to the sliding planes.

Tab. 3.11 Critical values of CTOD parameter in weld and at interface FL/HAZ

Location	12 O'clock		3 O'clock		6 O'clock	
	WCL	FL/HAZ	WCL	FL/HAZ	WCL	FL/HAZ
Critical CTOD value δ (mm)	0.56	1.08	0.67	1.06	0.59	1.07



-a-



-b-

Fig. 3.56 Fractography of fracture surfaces: a – in the vicinity of artificial fatigue crack initiation; b – in the vicinity of the crack tip opening displacement

The experimental results showed that the tested areas of the welded joint (welding and the interface between the fusion line and ZIT), present a significant reserve of plasticity, their fracture being ductile, and the stable extension of the crack occurs beyond the maximum loading (F_m). No brittle fracture or abrupt discontinuities (pop-in) were observed.

Chapter 4

RESISTANCE TO STRESS CORROSION CRACKING OF WELDED JOINTS

4.1. The experimental stand

Stress corrosion cracking occurs through the simultaneous action of a chemical environment and a static stress regime with at least a tensile effort and which leads to the intergranular or transgranular cracking of the material subjected simultaneously to the two types of actions [11],[39],[46],[48],[50],[60],[72],[101]. The onset of this phenomenon in hydrogen sulfide environment causes the metal material to be brittle by hydrogen atoms produced by acid corrosion in the surface area. The absorbed hydrogen is accelerated by the presence of sulfides, hence the fact that the sulfur content of the materials must be strictly controlled [44],[76],[83]. Hydrogen atoms can diffuse into the metallic material, reducing the ductility and toughness characteristics and increasing the susceptibility to cracking [3],[9],[13],[16],[21],[28],[32],[43],[45]. The corrosive medium used is hydrogen sulfide (H₂S) being the most common corrosive medium found in the transport of petroleum products and natural gas.

Stress corrosion cracking tests were performed under conditions of constant strain, materialized by means of bending pre-stressing devices under a certain angle. The specimens are of a flat strip type with welding perpendicular to the forces acting on them. The stress-strain combination is in the elastic field.

4.2. Experimental results

The dimensions of the specimen are shown in fig.4.4, and in fig.4.5 is shown the appearance of the specimen before the deformation.

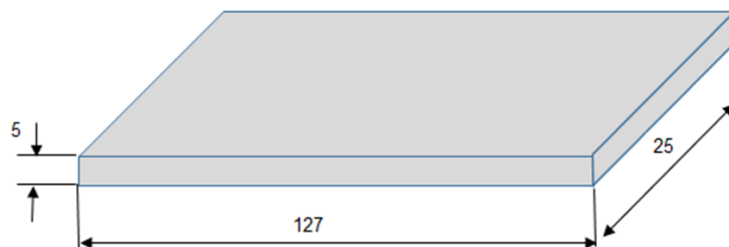


Fig.4.4 The shape and dimensions of the specimen



Fig.4.5 The image of the specimen before deformation

The values recorded at the end of the test are presented in tab.1

Tab.1 Values recorded

pH/H ₂ S	End of test values
pH	3.62
H ₂ S	3202 ppm

According to NACE TM 0177: 2016, the maximum pH value at the end of the test is 4. The test duration was 720 hours, and the temperature was maintained constant at 24°C ±3°C.

4.3. Metallographic examinations

In Figure 4.9 a, b and c are shown images of specimens (root, the middle and the top) at the end of the corrosion test.

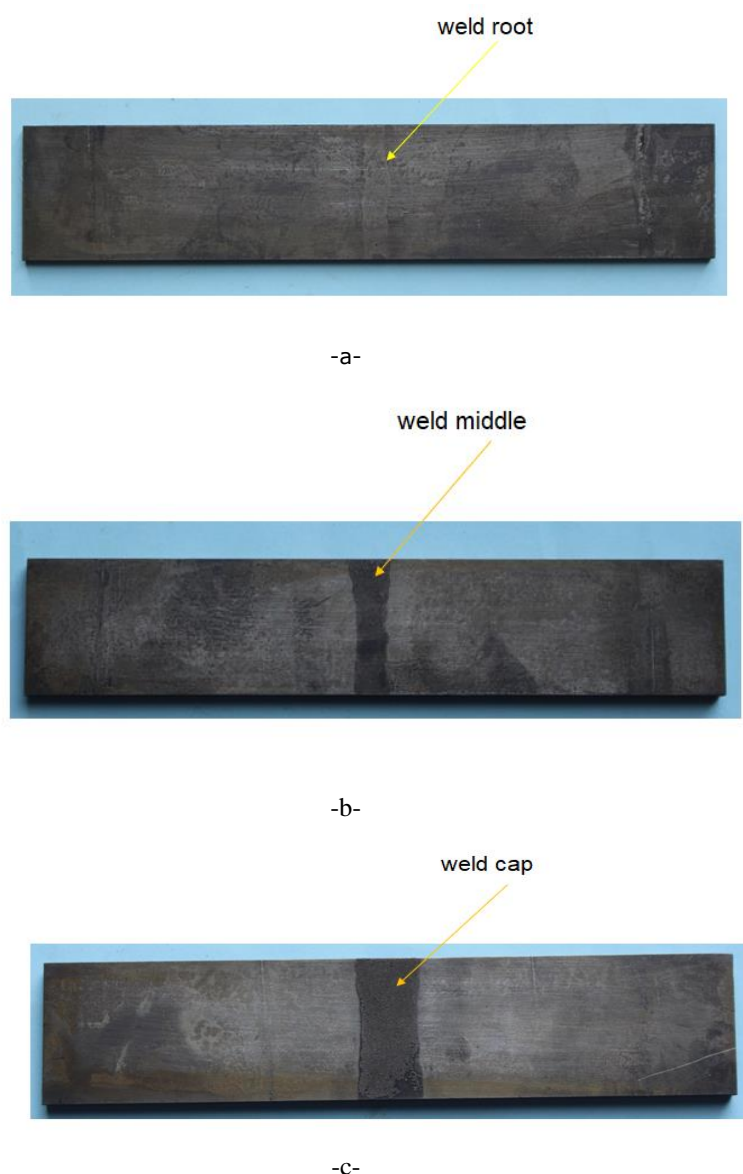


Fig.4.9 The appearance of the specimens at the completion of the corrosion test: a – weld root; b – weld middle; c- weld cap

The specimens subjected to stress corrosion cracking in hydrogen sulfide medium have a pH value of 3.62 with a H₂S concentration equal to 3202 ppm and no cracks were observed in the three welded joint areas.

Capitolul 5

NONDESTRUCTIVE EXAMINATION OF NARROW GAP MAG WELDING OF API 5L X65M THERMOMECHANICAL TREATED STEEL

5.1. Introduction

The nondestructive examination is one of the essential phases of pipeline welding. Determining the nature of the defects is particularly useful for identifying the causes and defining the measures to correct the execution or the technology.

Nondestructive control does not lead to deterioration of welded joints and does not negatively influence their behavior in service.

On the other hand, the destructive testing of welded joints is based on tests carried out with the destruction of the samples, respectively of the especially test pieces prepared. If by nondestructive control certain categories of defects can be determined, the values of the mechanical characteristics can be established only by destructive tests [22],[59],[81].

The nondestructive examination methods used in welded joints of API 5L X65M thermo mechanical treated steel, intended for the execution of underground and submarine pipelines having a diameter of 42 "(1066.8 mm) and a wall thickness of 31.75 mm were:

- visual examination;
- magnetic particle examination;
- radiographic examination (x-ray).

5.2. Visual examination

The external appearance of the welded joints using the technological parameters indicated in the papers [68],[69],[70] is presented in fig.5.4, and the aspect of the welded joint root, in fig.5.5.

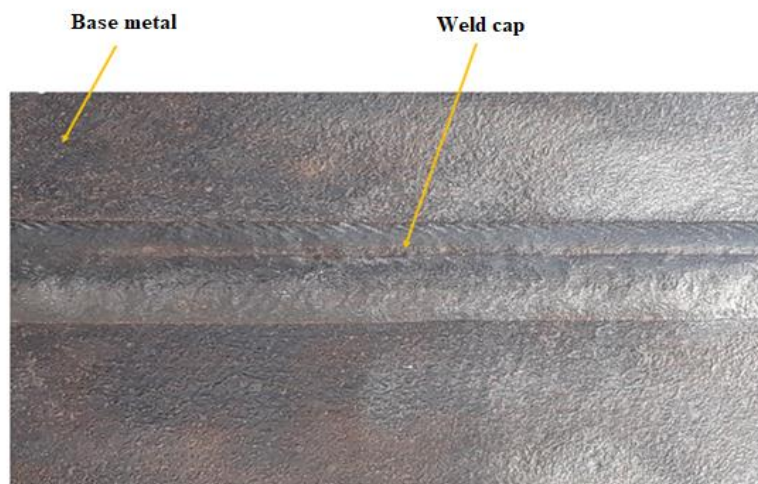


Fig. 5.4 External appearance of the welded joint

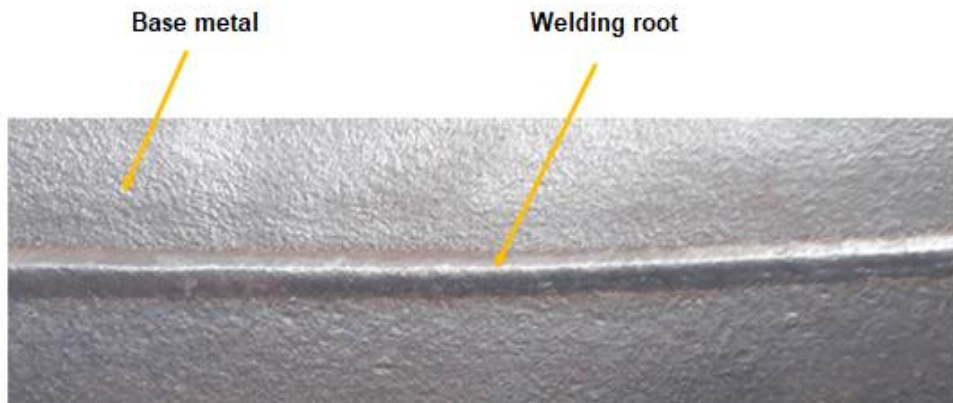


Fig. 5.5 Root welded joint

5.3. Magnetic particle examination

Magnetic particle control is a method of locating surface discontinuities or those that are in the immediate vicinity of the surface and can be applied only to ferromagnetic materials. In principle, this method of nondestructive control consists in the magnetization of the piece subject to control and the deposition on its surface of a fine ferromagnetic powder. In the areas where there are discontinuities, a magnetic field of dispersion or leakage will be formed due to the fact that the magnetic field lines will bypass the discontinuity, being forced to go outside the material of the piece [93]. The physical phenomenon that is disclosing the defect is the appearance of the dispersion field in the discontinuity area. Examination with magnetic powders, the wet method, using the magnetic yoke of the external pipeline welding is shown in fig.5.14.

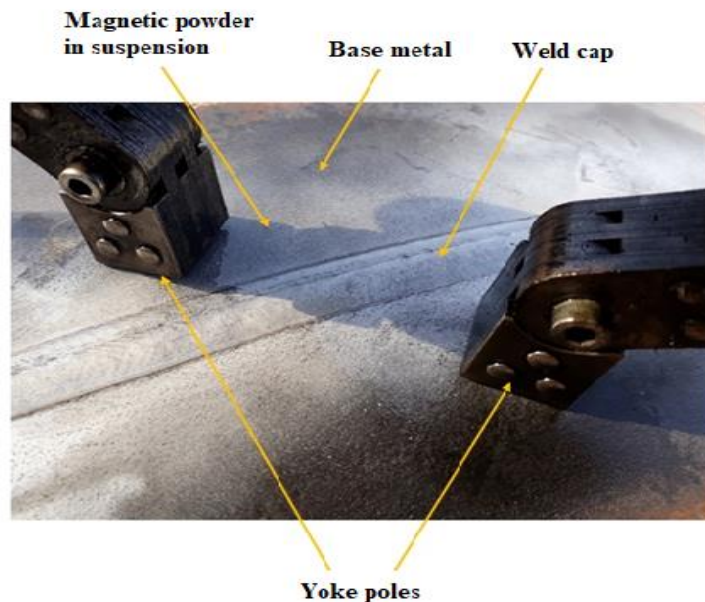


Fig. 5.14 Magnetic powder examination of pipes with 42" diameter and 31.75mm wall thickness

5.4. Radiographic examination (X-Ray)

The portable X-ray generator, C3003, is transported and controlled inside the pipes by the IRIS 10 X-Ray Crawler. The carrier assembly and the X-ray generator are shown in fig. 5.19.

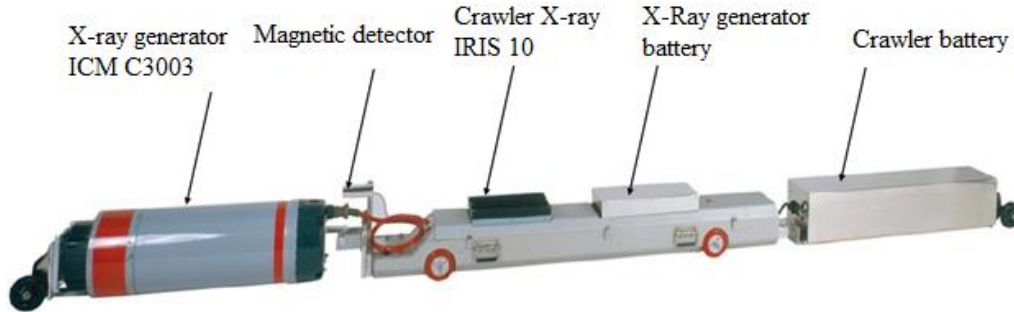


Fig. 5.19 The carrier assembly and X-ray generator IRIS 10

Table 5.2 shows the technical data of the radiography performed and in fig. 5.24 shows a radiographic film of the X-ray examination of the 42" x 31.75 mm pipe.

Tab. 5.2 Radiography technique sheet

Technical data	
Source	X - Rays
X-ray generator	ICM, type Sitex C3003
Focal spot	Ø5mm x 0.8mm
Material radiographed	API 5L X65M
Thickness	31.75mm
Diameter	42" (1066,8 mm)
Technique	SWSI
Source –film distance	533mm
Exposure time	3min.
KV	300KV
Cathodic current	3mA
Density	2.2 – 2.6
Film type	Kodak AA400
Sensitivity	1%
IQI Type	6 ISO 12
IQI position	Film side
Geometric unsharpness	0.31mm
Exposure	Panoramic
Acceptance standard	API 1104:2018

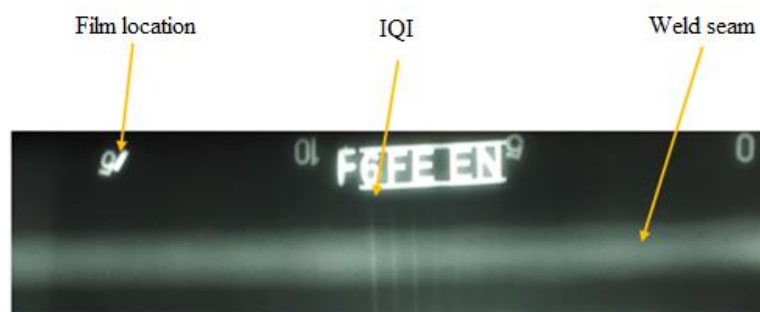


Fig. 5.24 X-ray film of the 42" x 31.75 mm pipeline

Chapter 6

GENERAL CONCLUSIONS AND ORIGINAL CONTRIBUTIONS. NEW RESEARCH DIRECTIONS

The doctoral thesis “**Contributions on the narrow gap MAG welding process of steels intended to gas pipelines execution**” aims to find a way to limit undesirable microstructural transformations in the areas of welded joints, while increasing productivity by implementing a special welding process of a thermo mechanically treated steel. The root pass & hot pass were made in the MAG version with spray arc, and the filling layers, in pulsed current, achieving a substantial increase in productivity by using both automatic internal root welding and by using two heads of welding to fill the joint. At the same time, a reduction in the consumption of filler materials is obtained, due to the narrow joint.

The main conclusions and original contributions of the paper can be summarized as follows:

1. The technological variant of MAG welding with narrow gap using an automatic welding equipment allows the use of a reduced heat input energy (2.97 - 5.67 kJ/cm) and welding speeds that reach values of 48 - 128 cm / min.
2. The execution of the root and hot passes in spray arc is opportune because due to the high melting power of the electric arc, defects such as lack of fusing at the root pass and between root and hot pass are avoided, defects that could occur due to the configuration of the welding joint (a shoulder of 1.27 mm with the gap of the joint, 0, mm).
3. The use of synergic pulsed current for the filling layers allows welding in difficult positions (vertically descending, overhead) as an effect of controlling the metal bath, by reducing its volume.
4. The selected base material, API 5L X65, is a thermo mechanically treated steel with high mechanical strength, with a lower degree of alloy compared to other steels in the normalized state, having the same mechanical strength characteristics. This is extremely beneficial for the metallurgical and technological behavior of this steel when welding.
5. The selected welding wires have a good compatibility with the basic material considered (API 5LX65) and to meet the condition of mechanical strength, they have a higher concentration in elements with hardening effect (C, Mn).
6. The experimental establishment of the optimal parameters of the narrow gap MAG welding process, led to the obtaining of welded joints without metal continuity defects (such as cracks, shrinkage cuts, slag inclusions and porosity) and a heat affected zone (HAZ) slightly extended.
7. The microstructure of the welded seam has a dendritic appearance with columnar orientation of the crystalline grains, and the HAZ consists of a ferritic matrix with small amounts of bainite and carbonitrides of the alloying elements.
8. The hardness gradient on the cross section of the welded joints demonstrates that the experimentally established thermal regime parameters prevent the softening of the heat affected zone (HAZ) and ensure good mechanical properties.
9. The results of the charpy impact test show that at the lowest test temperature, (-50°C), the

absorbed energy KV of the upper and lower part of the deposited metal exceeds the minimum value, of 38 J, imposed by the norm specific to this basic material.

10.The fracture surface of the toughness measuring specimens has a matte-fibrous appearance, and its character is ductile, characterized by a low speed of movement of the crack, respectively by high values of the energy absorbed for its propagation.

11.For the experimental conditions used, the tensile strength of welded joints values, $R_m = 576 \dots 598 \text{ N/mm}^2$, are higher than those required for the base material, $R_m \geq 535 \text{ N/mm}^2$.

12.Narrow gap MAG welded joints in pulsed current and multiple layers, made of thermo mechanically treated steel, X65M, have a high capacity of plastic deformation, proven by the absence of cracks in the seam until the bending angle of 180° is reached.

13.The results of the fracture mechanics tests showed that the tested areas of the welded joint (welding and the interface between the fusion line and ZIT), show a significant reserve of plasticity, their fracture being ductile and the stable expansion of the crack takes place beyond the maximum load (F_m).No fragile fracture or abrupt discontinuities were observed, and the displacement values at the opening of the crack tip are much higher than those specified in the rules used in the manufacture of underground and submarine oil and gas pipelines.

14.The stress corrosion cracking in hydrogen sulfide medium revealed a pH value of 3.62, an H_2S concentration equal to 3202 ppm and the absence of cracks in the three areas of the welded joints.

15.Visual and magnetic particle inspection, together with X-ray examinations, on the entire thickness of the welded joints did not identify any defects specified in the internationally imposed standards for these products.

In conclusion, it can be shown that the approach and solution within the proposed limits of the research topic that is the subject of the doctoral thesis, by systematic follow-up, highlighting and scientific substantiation of the transformations that occur in narrow gap MAG welding, where the root pass & hot pass were executed in the MAG version with spray arc, and the filling layers, in pulsed current, represent an original contribution.

Combining the research of the applied side of these investigations in terms of the level of mechanical properties obtained with the phenomenological side, the determination and scientific explanation of the features that define the metallurgical and technological welding behavior of thermomechanically treated steels and justifies the improvement of welded joints, makes the thesis to be in line with modern trends and methodology used in scientific research.

Future research directions:

- the opportunity of laser welding of thermomechanically treated steels;
- laser brazing, which will minimize the mixing of materials, the process being based on the diffusion of interfaces between the molten filler material and the base material.

Bibliography:

1. Adonyi Y. 2006, Heat affected zone characterization by physical simulations, *Welding Journal*, Vol.85, Issue 10, pp 27-42.
2. Anderson, T L: *Fracture Mechanics – Fundamentals and Applications*. Second Edition, CRC Press, Boca Raton, Florida, USA, 1995, pp.1-680.
3. Arzola S., Mendoza-Flores J., Duran-Romero R., Genesca J. 2006, Electrochemical Behavior of APIX70 Steel in Hydrogen Sulfide-Containing Solutions. *Corrosion* 62 (2006) 433-443.
4. Babkin and Gladkov 2016 Identification of Welding Parameters for Quality Welds in GMAW, *Welding Journal* 95, 37-46.
5. Banerjee K. Improving weldability of an advanced high strength steel by design of base metal microstructure. *Journal of Materials Processing Technology* 229 (2016) 596–608.
6. Bang K.S., Kim W.Y., Estimation and prediction of HAZ soft-ening in thermomechanically controlled - rolled and accelerated - cooled steel. *Welding Journal* 81, 8, 2002, 174-179.
7. Bao Y.and Wierzbicki T. On fracture locus in the equivalent strain and strain triaxiality space, *International Journal of Mechanical Science*, 46, 2004,81-98.
8. Barthel C., Klusemann B., Denzer R.,Svendson B. . Modeling of a thermomechanical process chain for sheet steels. *International Journal of Mechanical Sciences* 74 (2013) 46–54.
9. Bordeasu I., Popoviciu M.O., Mitelea I., Balasoiu V., Ghiban B., Tucu D., Chemical and mechanical aspects of the cavitation phenomena, *Rev.Chim. (Bucharest)*, 58, no.12, 2007, pp.1300-1304.
10. Burca M., Negoitescu S., *Sudarea MIG-MAG*, Editura Sudura Timisoara 2004, pp.1-224.
11. Burduhos-Nergis D.P, Carmen Nejneru C., Burduhos-Nergis D.D, Savin C., Sandu V.S., Toma S.L., Bejinariu C., The Galvanic Corrosion Behavior of Phosphated Carbon Steel Used at Carabiners Manufacturing, *Rev.Chim (Bucharest)*,70,no.1, 2019,pp.215-219.
12. Burgold A., Henkel S., Roth S., and Kuna M., Bierman H.: Fracture mechanics testing and crack growth simulation of highly ductile austenitic steel, *Materials Testing* 60 (2018) No.4 pp.341-348.
13. Cendales E.D., Orjuela F.A. and Chamarravi O., Computational modeling of the mechanism of hydrogen embrittlement (HE) and stress corrosion cracking (SCC) in metals, *Journal of Physics*,2016, 687.
14. Coelho SR et al 2013 *Journal Materials Science & Engineering A* 578, 125.
15. Coelho R.S.,Corpas M. , Moreto J.A. ,Jahnc A. , Standfuß J. , Kaysser-Pyzalla, Pinto A.H. Induction-assisted laser beam welding of a thermomechanically rolled HSLA S500MC steel: A microstructure and residual stress assessment. *Materials Science & Engineering A* 578 (2013) 125–133.
16. Costa Mattos H., Bastos I. and Gomes C. 2014 *Corrosion Science* 80, 143.
17. Dawes, M G.: *Elastic-Plastic Fracture Toughness based on COD and J-contour Integral Concepts in Elastic-Plastic Fracture*. ASTM STP 668, American Society for Testing and Materials, 1979. pp 307-333.
18. Deheleanu D., *Sudarea prin topire*, Editura Sudura Timisoara 1997, pp.198.
19. Ding W.H., Research and Development into Low Temp Toughness of Heavy Wall X80 at Shougang. 9th International Conference on Pipeline. Calgary 2012, 117-121.
20. Dobrota D., Corrosion of Welded Metal Structures of Mining Equipment, *Rev.Chim (Bucharest)*, 69, no.9, 2018, pp.2563-2566.
21. Domizzi G., Anteri G. and Ovejero Garcia J., *Corrosion Science* 43, 2001, 325-339.

22. Dong Su Bae, Sang Pill Lee, Joon Hyun Lee : Evaluation on defect in the weld of stainless steel materials using nondestructive technique. *Fusion Engineering and Design*, Vol. 89, Issue 7 – 8, October 2014, pp. 1739 – 1745.
23. Faiz F., Mustafa I. Rao, Automatic Welding Machine for Pipeline Using MIG Welding Process, *International Research Journal of Engineering and Technology*, Vol.3, Dec.2016.
24. Garcia K.E., Morales A.L., Barrero C.A., Greneche J.M.: New contributions to the understanding of rust layer formation in steels exposed to a total immersion test. *Corrosion Science* Vol.48, 2006, pp. 2813 – 2830.
25. Gholamreza K., Hesam P. , Mohammad R. J., Abbas G. ,Microalloyed steel welds by HF-ERW technique: Novel PWHT cycles, microstructure evolution and mechanical properties enhancement *International Journal of Pressure Vessels and Piping* 152 (2017) 15-26.
26. Ghosha S. , Singha A.K. , Mulaa S., Chandab P. , Mahashabdeb V.V. , Royb T.K. Mechanical properties, formability and corrosion resistance of thermomechanically controlled processed Ti-Nb stabilized IF steel. *Materials Science & Engineering A* 684 (2017) 22–36.
27. Gong P., Palmiere E.J, Rainforth W.M. Dissolution and precipitation behavior in steels micro alloyed with niobium during thermo mechanical processing. *Acta Materialia* 97 (2015) 392–403.
28. Guo H. and He X., Electrochemical Study on Corrosion Behavior of X70 Steel in Weakly Acidic Solutions Containing H₂S, 2006, *Journal Corrosion & Protection*, (05):232:236.
29. Hedia H.S., Shabara M.A., Fattah A.A and Helal M.M. 2005, Effect of Crack Configuration and Pre-Crack Length on Stress Intensity Factors, *Journal of material prufung* 47 10 2-7.
30. Hildebrand J., Werner F., Change of structural condition of welded joints between high-strength fine-grained and structural steels, *Journal of civil engineering and management*, 2, 2004,87-95.
31. Irwin G.:Analysis of stresses and strains near the end of a crack traversing a plate. *Journal of Applied Mechanics* 24 (1957), pp.361–364.
32. Jafari, S., Harandi S.E., Singh Raman R.K.: A Review of stress-corrosion cracking and corrosion fatigue of magnesium alloys for biodegradable implant applications. *J. Mater.* Vol. 67, 2015, pp. 1143–1153.
33. Jeong S., Park G.,Kim B., Moon J., Park J. and Lee C. Precipitation behavior and its effect on mechanical properties in weld heat – affected zone in age hardened FeMnAlC lightweight steels. *Journal Materials Science and Engineering A*. 2019 Vol. 742, pp. 621 – 68.
34. Kannan M.B., Dietzel W.: Pitting-induced hydrogen embrittlement of magnesium-aluminum alloy. *Mater. Des.* 2012, Vol. 42, pp. 321–326.
35. Kang Zhou, Ping Yao: Overview of recent advances of process analysis and quality control in resistance spot welding. *Mechanical Systems and Signal Processing*, Vol. 1241, June 2019, pp. 170-198.
36. Karadeniz E., Ozsarac U. and Yildiz C., The effect of process parameters on penetration in gas metal arc welding processes, *Journal of materials and design* 28, 2005.
37. Kim H., Ki H.,Moon, In J., Kim W. Ki, Park G. B. and Lee S. K. Influence of carbon equivalent value on the weld bead bending properties of high – strength low – alloy steel plates. *Journal of Materials Science &Technology*.2017.Vol. 33, Issue 4, pp. 321 – 329.
38. Kim W.K., Koh S.U., Yang B.Y. and Kim K.Y., *Corrosion Science and Technology* Vol.6, No.3, 2007, 96-102.

39. Kisaka Y. and Gerlich A. 2016 Review and critical assessment of hardness criterion to avoid sulfide stress cracking in pipeline welds, ASME Pressure Vessels and Piping Conference 6B, Vancouver, Canada.
40. Krampit A.G., Krampit N.U., Krampit M.A. Mechanical properties of welded joint in welding with pulsed arcs, *Applied Mechanics and Materials*, Vol.379 (2013) 195-198.
41. Laitinen R., Porter D.A., Karjalainen L.P., Leiviska P. and Komi J., 2013 Physical Simulation for Evaluating Heat Affected Zone Toughness of High and Ultra High Strength Steels , *Materials Science Forum* Vol.762, 711-716.
42. Liangyun L., Konga X., Hua Z., Qiub C., Zhao D., Dub L.. Hydrogen permeation behavior in relation to microstructural evolution of low carbon bainitic steel weldments. *Corrosion Science* 112 (2016) 180–193.
43. Lupescu S., Corneliu Munteanu C., Istrate Earar K., The Influence of Zr on Microstructure, Mechanical Properties and Corrosion Resistance in Mg-Y-Zr Biodegradable Alloys, *Rev.Chim (Bucharest)*,69, no.12, 2018, pp.3382-3385.
44. Ma H., Cheng X., Li G., Chen S., Quan Z., Zhao S., Niu L. 2000 The Influence of Hydrogen Sulfide on Corrosion of Iron Under Different Conditions. Pergamon. *Corrosion Science* 42, 1669-1683.
45. Melchers E.R., Paik K.J.: Effect of tensile strain on the rate of marine corrosion of steel plates. *Corrosion Science*, Vol. 52, Issue 10, 2009, pp. 2298 – 2303.
46. Mitelea I., Bordeasu I., Popoviciu M.O., Hadar A., Corrosion of stainless steels with “soft”martensitic structure, *Rev.Chim (Bucharest)*, ,58,no.2,2007,pp.254-57.
47. Mitelea I., Simionescu D., Craciunescu M.C. and Utu I.D. : Fracture toughness of MAG welds in pulsed current of API5L X65M thermomechanical treated steel *Material Testing* 62 (2020) 3, pp.304-310.
48. Mitelea I., Simionescu D., Bordeasu I., Susceptibility to Stress Corrosion Cracking in Hydrogen Sulfide Environment of MAG Welded Joints of API 5L X65M Thermomechanical Treated Steel, *Rev.Chim (Bucharest)*, 70 no.12, 2019, pp.4405-4410.
49. Moore P., Pisarski H.: Validation of methods to determine CTOD from SENT specimens, *Proceedings ISOPE-2012,of the 22nd International Offshore (Ocean) and Polar Engineering Conference*, Rhodes, Greece,(2012), pp.1-8.
50. Nazarova M.N., Akhmetov R.R., Krainov S.A. Temperature factors effect on occurrence of stress corrosion cracking of main gas pipeline. *Earth and Environmental Science* 87, 2017.
51. Nie Y., Shang C., Song X, etal. Properties and homogeneity of 550MPa grade TMCP steel for ship hull (J).*Metallurgy and Materials*, 2010, 17(2): 179-184.
52. Nishioka K. Market requirements of thermomechanically processed steel for the 21st century, *Steel World* 2000, vol.5, no.1, pp. 61-67.
53. Nishioka K.and Ichikawa K. Progress in thermomechanical control of steel plates and their commercialization. *Science and Technology of Advanced Materials*, 13, 2012.
54. Oh C.K, Kim Y.J., Park J.M., Baek J.H. and Kim W.S.2007, Development of stress modified fracture strain for ductile failure of API X65 steel, *International Journal Fracture*, 143, 119-33.
55. Opiela M., Elaboration of thermomechanical treatment conditions of Ti-V and Ti-Nb-V microalloyed forging steels, *Archives of Metallurgy and Materials* 2014, vol.59, issue 3, pp. 1181-1188.
56. Paul A.and Mark C., *CRC Evans Automatic Welding USA, World of pipelines*, Vol. 14, 2014.
57. Perez N. *Fracture Mechanics 1st Ed.* (Boston: Kluwer Academic Publishers), 2004,47-96.

58. Poznyakov V., Jdanov S., & Maksimenko A. (2012). Structure and properties of welds made from S355J2 steel. *Automat Weld*, 8, 7-11.
59. Raju D.T. and Shanthi K., Analysis on x-ray parameters of exposure by measuring x0-ray tube voltage and time of exposure ,*The International Journal of Engineering and Science*, Volume 3, Issue 6, 2014, pp 69-73.
60. Ralston K.D., Williams G., Birbilis N.: Effect of pH on the grain size dependence of magnesium corrosion. *Corrosion*, Vol. 68, 2012 pp. 507–517.
61. Robert Andrews, Harry Kamping, Henk de Haan, Otto Jan Huising and Neil Milwood. Guidance for mechanized GMAW of onshore pipelines. *The Journal of Pipeline Engineering*, Vol. I 2, No.4, 2013
62. Safta V. *Defectoscopie Nedistructiva Industriala*. Editura Sudura, 2001.
63. Safta V.I and Safta V.I, *Incarcarile tehnologice si de rezistenta ale imbinarilor sudate sau lipite*. Editura Sudura Timisoara, 2006, pp.1-339.
64. Scotti A., Ponomarev V., Lucas W. 2012, A scientific application oriented classification for metal transfer modes in GMA welding, *Journal of Materials Processing Technology* 212(6), 1406.
65. Shen G. and Tyson W. R. Evaluation of CTOD from J-integral for SE(T) specimens, *Proceedings of the Pipeline Technology Conference*, Ostend, Belgium (2009), pp.1-6.
66. Shin S.Y., Hwang B., Lee S., Kim N. J., Ahn S.S.2007 Correlation of microstructure and charpy impact properties in APIX70 and X80 line pipe steels. *Materials Science and Engineering*: A458 281-9.
67. Siciliano F., *Modern High Strength Steels for Oil and Gas Transmission Pipelines*. 7th International Conference on Pipeline, Calgary 2008, 29-35.
68. Simionescu D., Mitelea I., Burcă M.: Opportunities of narrow gap MAG welding of API 5L X65M steel pipeline, *Proceedings of the 26th International Conference on Metallurgy and materials*, METAL 2017, Brno, Czech Republic, pp.699-704.
DOI:10.1088/1757-899X/416/1/012008.
69. Simionescu, D., Mitelea I., Burca M., Utu I.D. Mechanical behavior of narrow gap MAG welding of API 5L X65M steel pipeline. *IOP Conference Series: Materials Science Engineering* 416 (2018) pp.1-8.
DOI: 10.1088/1757-899X/416/1/012008.
70. Simionescu D., Mitelea I. and Burca M., Utu I.D.: Cold bending characteristics of MAG pulse welding of API 5LX65 thermomechanical treated steel. *Metal 2019*, International Conference on Metallurgy and Materials, published 2019, pp.532-539
71. Srinivasa R.,Gupta O.P., Murty S.S. and Rao A. 2009, Effect of process parameters and mathematical model for the prediction of bead geometry in pulsed GMA welding, *The International Journal of Advanced Manufacturing Technology* , 45 (5-6), 496-505.
72. Strobl Sau: *Stress Corrosion Cracking*. *Pract. Metallogr.* Vol.54, Issue.3, 2017, pp. 153 – 162.
73. Viggo T. and Needleman A., Analysis of the Charpy V-notch test for welds. *Engineering Fracture Mechanics* 65, no.6, 2000, 627-643.
74. Wang W., Shan Y.Y., Yang K. Study of High Strength Pipeline Steels with Different Microstructures. *Materials Science and Engineering A*, 2009, 502:38-44.
75. Wells, A. A.: Unstable crack propagation in metals: cleavage and fast fracture. *Proceedings of the crack propagation symposium*, Vol.2, Cranfield, UK (1961) pp.210-230.
76. Winzer N., Atrens A., Song G., Ghali E., Dietzel W., Kainer K.U., Hort N., Blawert C. : A critical review of the stress corrosion cracking (SCC) of magnesium alloys. *Adv. Eng. Mater.* 2005, Iss.7, pp. 659–693.

77. Xin Q. 2007, The Study of Microstructure and Mechanical Properties for Pipeline-Steel X65 (Liaoning: University of Science and Technology).
78. Xu W.H., Lin S., Fan C.L., Ynag C.L. Prediction and optimization of weld bead geometry in oscillating arc narrow gap all-position GMAW welding. *International Journal Advance Manufacturing Technology*, 2014, 72, 1705-1716.
79. Yajima , 'Extensive Application of TMCP-manufactured High Tensile Steel Plates to Ship Hulls and Offshore Structures' *Mitsubishi Heavy Industries Technical Review* vol. 24, no. 1, February 1987.
80. Yapp D. and Blackman S.A., Recent Developments in High productivity Pipeline Welding, 2004, Vol. XXVI, No. 1/89.
81. Yiming Huang, Dejin Zhao, Huabin Chen, Lijun Yang, Shanben Chen : Porosity detection in pulsed GTA welding of 5A06 Al alloy through spectral analys. *Journal of Materials Processing Technology*, Vol. 259, September 2018, pp. 332-340.
82. Zhang M.C., Yang K., Shan Y.Y. The Effect of Thermo-mechanical Control process in Microstructures and Mechanical Properties of a Commercial Pipeline Steel. *Materials Science and Engineering A.*, 2002, 225:14-20.
83. Zhang T. et al 2017 *International Journal of Hydrogen Energy* 42(39) 25 102.
84. Zhou M, Du L, Liu X 2011 *Journal of Iron and Steel Research, International* **18(3)** 59.
85. Zhu X. and Joyce J.A. *Engineering Fracture Mechanics* 2012, 85:1-46.
86. Ziad M., Frédéric R., Ngoc T. T. Theoretical and numerical modeling of the thermomechanical and metallurgical behavior of steel. *International Journal of Plasticity* 27 (2011) 414–439.
87. XXX ANSI/NACE MR0175/ISO 15156:2015, Petroleum, petrochemical and natural gas industries – Materials for use in H₂S containing environments in oil and gas productions.
88. XXX ANSI/NACE TM-0177: 2016. Laboratory Testing of Metals for Resistance to Sulfide Stress Cracking and Stress Corrosion Cracking in H₂S Environments.
89. XXX API 1104, Welding of Pipelines and Related Facilities, Twenty-First Edition, 2013.
90. XXX API Specification 5L, Specification for Line-Pipe, Forty-Sixth Edition, 2018.
91. XXX ASME Boiler and Pressure Vessel Code Sect.V. Nondestructive Examination, 2017.
92. XXX ASME Boiler and Pressure Vessel Code Sect.II Part C. Specifications for Welding Rods, Electrodes and Filler Metals, 2017.
93. XXX ASM Metals Handbook Vol.17 1989. Nondestructive Evaluation and Quality Control
94. XXX ASTM A370-13, Standard Methods and Definitions for Mechanical Testing of Steel Products.
95. XXX ASTM E8-16, Standard Test Methods for Tension Testing of Metallic Materials.
96. XXX ASTM E23-12, Standard Test Methods for Notched Bar Impact Testing of Metallic Materials.
97. XXX ASTM E190-14, Standard Test Method for Guided Bend Test for Ductility of Welds.
98. XXX ASTM E384-11, Standard Test Method for Knoop and Vickers Hardness of Materials.
99. XXX ASTM E1290-08: Standard Test Method for Crack-Tip Opening Displacement (CTOD) Fracture Toughness Measurement (Withdrawn 2013). American Society for Testing and Materials, 2008.
100. XXX ASTM E1820 - 11: Standard Test Method for Measurement of Fracture Toughness. American Society for Testing and Materials, 2011.
101. XXX ASTM G30-97(2016), Standard Practice for Making and Using U-Bend Stress-Corrosion Test Specimen.

102. XXX ASTM G39:2011. Standard Practice for Preparation and Use of Bent-Beam Stress-Corrosion Test Specimens.
103. XXX American Welding Society, Welding Handbook, Volume 2, Welding processes, Part 1, Ninth Edition, p.159.
104. XXX American Welding Society, Welding Handbook, Volume 4, Materials and Applications, Part 1, Ninth Edition, p.41.
105. XXX BS 5762:1979: Methods for crack opening displacement (COD) testing. British Standards Institution, 1979.
106. XXX BS 7448-1:1991: Fracture mechanics toughness tests: Part 1: Method for determination of K_{Ic} , critical CTOD and critical J values of metallic materials. British Standards Institution, 1991.
107. XXX BS 7910:2005: Guide to methods for assessing the acceptability of flaws in metallic structures. British Standards Institution, 2005, pp.1-306.
108. XXX BS EN ISO 15653-2010: Metallic materials - Method of test for the determination of quasistatic fracture toughness of welds. British Standards Institution, 2010.
109. XXX DNVGL-ST-F101:2017. Submarine Pipeline Systems. Det Norske Veritas Germanischer Lloyd, pp.1-521.
110. XXX EN10208:2009: Steel pipes for pipelines for combustible fluids. Technical delivery conditions.
111. XXX Instron da/dN Crack Propagation Software for Instron 8800 Systems (version 32).
112. XXX Instron K1C Fracture Toughness Software for Instron 8800 Systems (version 32).
113. XXX ISO 12135:2002: Metallic materials - Unified method of test for the determination of quasistatic fracture toughness. International Standards Organization, Geneva, Switzerland (2008), pp.1-7.
114. XXX TWI – Are TMCP steels readily weldable?, Material preluat de pe internet de la adresa www.twi-global.com.